nature photonics

SUPPLEMENTARY INFORMATION

DOI: 10.1038/NPHOTON.2012.110

Supplementary information

Avalanche amplification of a single exciton in a semiconductor nanowire

Gabriele Bulgarini,[1,*] Michael E. Reimer,[1,†] Moïra Hocevar,[1] Erik P.A.M. Bakkers,[1,2] Leo P. Kouwenhoven,[1] and Valery Zwiller[1]

[1]*Kavli Institute of Nanoscience, Delft University of Technology, The Netherlands*

[2]*Eindhoven University of Technology, The Netherlands*

*Electronic address: `g.bulgarini@tudelft.nl`

†These authors contributed equally to this work

© 2012 Macmillan Publishers Limited. All rights reserved.

 DOI: 10.1038/NPHOTON.2012.110

Single quantum dot spectroscopy

Photocurrent spectroscopy has been utilized for determining quantum dot absorption transitions. The observed absorption spectra has been compared to typical photoluminescence spectroscopy of individual InAsP quantum dots in intrinsic InP nanowires in order to attribute absorption peaks to transitions in the quantum dot energy levels. Typical photoluminescence spectra as a function of excitation laser power are shown in Supplementary Figure 1 and exhibit the sequential s-, p-, and d-shell filling as the excitation power is increased. The constant energy separation between observed shells, suggests a 2D parabolic in-plane potential as a valid approximation for quantum dots in nanowires. This approximation has been used to calculate the quantum dot diameter (27 nm).

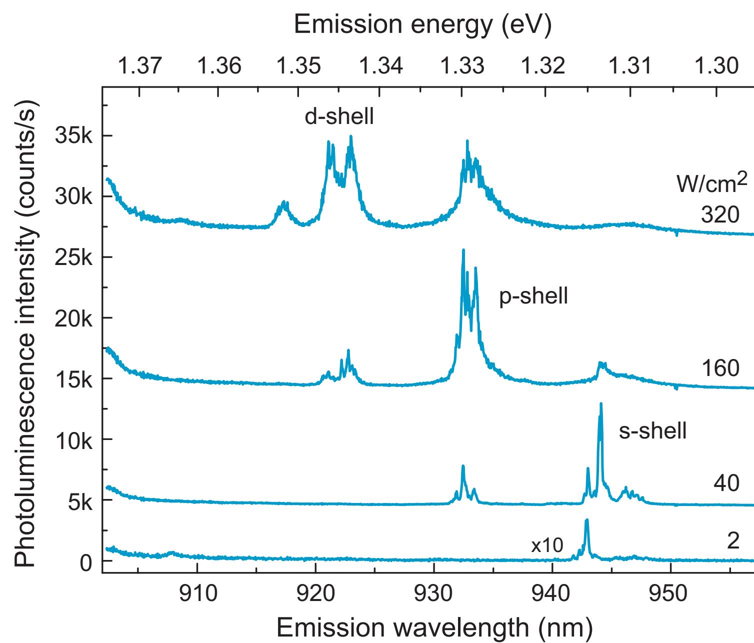

Figure 1: Photoluminescence spectroscopy of a single InAsP quantum dot in an InP nanowire. As a function of increasing laser excitation power, we observe the sequential filling of the quantum dot s-, p-, and d-shell with a constant energy separation between the shells.

© 2012 Macmillan Publishers Limited. All rights reserved.

Photodiode internal quantum efficiency

The internal quantum efficiency (IQE) of a photodiode is defined as the ratio between charges to absorbed photons when the internal gain is not active. We measured the internal quantum efficiency of our nanowire photodiode at $V_{sd} = 0\,\mathrm{V}$ where only the p-n junction built-in electric field separates electron-hole pairs and charge carriers do not gain enough energy to initiate avalanche multiplication. Under illumination, the current-voltage characteristic of the nanowire photodiode shows a negative saturation current (I_{sc}). The dark current of the device is subtracted to the saturation current in order to obtain the net number of charge carriers generated by photon absorption (Supplementary Figure 2a). We observe a linear dependence of the saturation current with the excitation power, resulting in an internal quantum efficiency of 96 % (Supplementary Figure 2b). Additionally, we observe under illumination an open-circuit voltage ($V_{oc} = 0.5\,\mathrm{V}$), which is constant for the investigated range of excitation power.

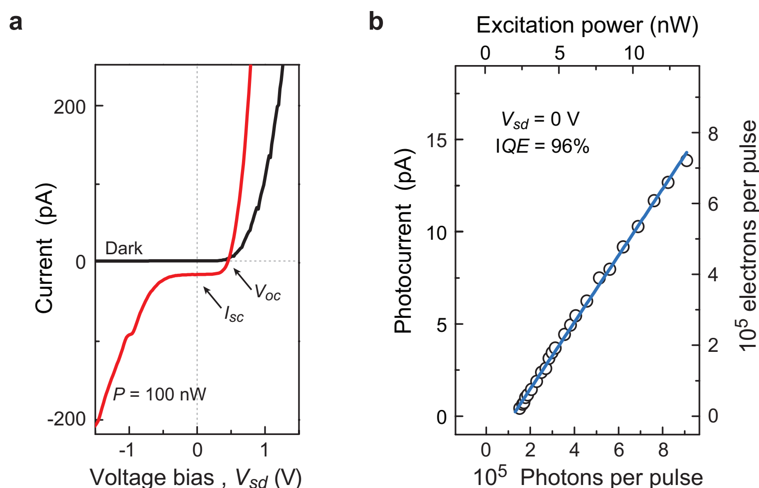

Figure 2: Internal quantum efficiency. **a**, Current-voltage characteristic in dark (black) and upon above-bandgap illumination (red). We observe an open-circuit voltage $V_{oc} = 0.5\,\mathrm{V}$ and photocurrent at $V_{sd} = 0\,\mathrm{V}$, without multiplication gain. **b**, By varying the incident power, we determine an efficiency (IQE) of 96 % for the absorbed photon to collected charge conversion.

© 2012 Macmillan Publishers Limited. All rights reserved.

DOI: 10.1038/NPHOTON.2012.110

Avalanche breakdown

In Supplementary Figure 3, we analyze the breakdown behavior of the nanowire photodiode in dark at room temperature. The black curve exhibits the occurrence of a 'hard-knee' abrupt increase of the current at V_{sd} = -15 V, typical of an avalanche breakdown. Subsequently to the breakdown, we slowly sweep the applied bias to V_{sd} = 0 V and measure again the dark characteristic of the device, utilizing the same bias sweep rate and direction. We observe the characteristic of the device to be dramatically changed by the reach of the breakdown voltage. The avalanche breakdown shifts to higher reverse bias and becomes less sharp (red curve) until turning into a smooth Zener-like breakdown (blue curve). We attribute this degradation of the photodiode characteristics to diffusion of dopants caused by heat in the nanowire at the breakdown field and consequent change of the doping profile along the nanowire. Thus, in order to preserve the quality of the device, we operate the nanowire photodiode in sub-Geiger operation, below the avalanche breakdown voltage.

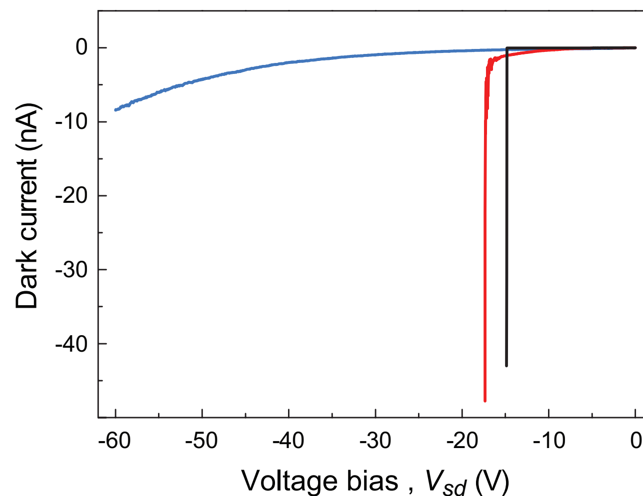

Figure 3: Avalanche breakdown in an InP nanowire p-n junction. The occurrence of an avalanche breakdown is observed at V_{sd} = -15 V in the photodiode dark current (black). The nanowire properties change after reaching the breakdown. First, the avalanche breakdown shifts to higher reverse bias and becomes less sharp (red curve) and subsequently, turns into a smooth Zener-like breakdown (blue curve). The three curves are measured subsequently, under the same bias sweep rate and direction.

© 2012 Macmillan Publishers Limited. All rights reserved.

DOI: 10.1038/NPHOTON.2012.110

Signal-to-noise ratio temperature dependence

The reported photodetection measurements have been performed at a temperature of 40 K, where the photocurrent signal-to-noise ratio (SNR) is observed to be maximum, as shown in Supplementary Figure 4a. The SNR has been measured using green laser excitation with an optical power of 5.6 fW incident on the sample, equivalent to an estimated flux of one photon absorbed per excitation pulse at 120 Hz. Cooling down the device below 40 K results in a reduction of the SNR. This reduction can be explained by dopant freezing which decreases the electric field across the p-n junction. To support this explanation, current-voltage measurements in dark as a function of the temperature are shown in Supplementary Figure 4b. The forward bias current of the photodiode presents an abrupt decrease at about 40 K, which is most likely a result of dopant freezing, thus diminishing the p-n junction electric field and increasing the photodiode resistance. By fitting the dark current-voltage curve at 40 K with a diode characteristic, we obtain a total series resistance of 60 MΩ.

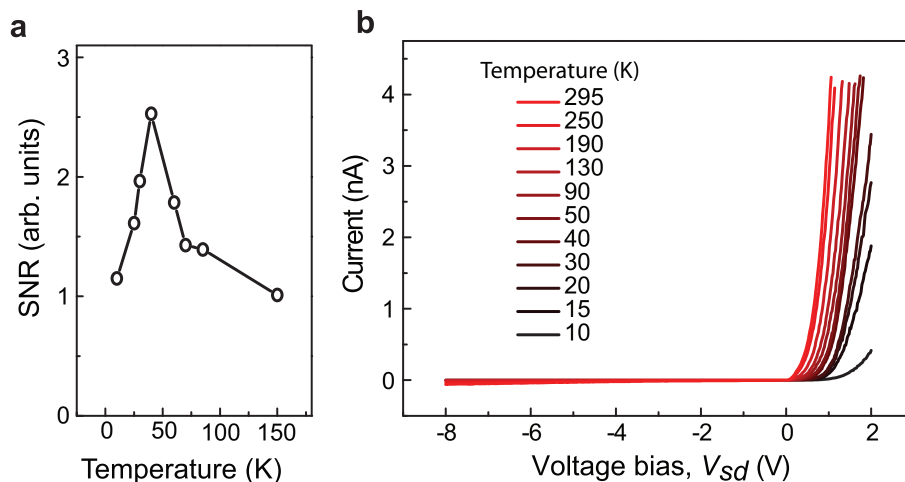

Figure 4: a, Signal-to-Noise Ratio (SNR) of the nanowire photodiode as a function of temperature measured for an optical power of 5.6 fW incident on the sample. We measure the maximum SNR (2.5) at 40 K. This temperature has been used for photocurrent measurements in the few-photon regime. **b**, Electrical characteristics of the photodiode in dark as a function of the operating temperature from 295 K to 10 K. Cooling down the photodiode below 40 K produces a dramatic decrease of the forward bias current, which is attributed to dopant freezing in the nanowire.

© 2012 Macmillan Publishers Limited. All rights reserved.

DOI: 10.1038/NPHOTON.2012.110

Photon counting measurements

Our estimations of the absorbed photon rate are confirmed by photocurrent measurements performed in the few-photon regime. We measure the current after individual excitation pulses at 120 Hz and we plot in Supplementary Figure 5a the statistical distribution of the current, using a bin size of 0.1 pA. Data are presented for dark and under laser excitation with an estimated average absorbed photon rate, $n = 1.00$, 2.14 and 4.29. Indeed, the addition of a single absorbed photon results in discrete steps of 0.4 pA for the current distribution and broadening at higher photon number consistent with Poisson statistics. The discrete step size of 0.4 pA is in very good agreement with the measured gain, as the estimated current for a single photon is:

$$I = G_i \times e \times f = 2.3 \cdot 10^4 \times e \times 120\,\mathrm{Hz} = 0.44\,\mathrm{pA}. \tag{1}$$

G_i is the multiplication internal gain, f is the repetition frequency of the laser excitation and e is the electron charge.

The current distributions are well fitted by a sum of Gaussian peaks that are equally spaced by 0.4 pA and have the same width. Single Gaussian peaks are displayed in yellow and the final fit functions are displayed by colored lines. The formula used for the fit is:

$$\sum_{0}^{k} A_k \times e^{-(x-x_0-k\cdot\mu)^2/2\sigma^2}. \tag{2}$$

Gaussian peaks are centered at multiple integers (k) of the photocurrent obtained by a single photon absorption event, $\mu = 0.4\,\mathrm{pA}$. The offset x_0 is given by the background drift current of the p-n junction (0.48 pA). The variance of the peaks (σ^2) is determined by the noise fluctuation measured in the dark (0.2 pA) and kept fixed for all Gaussian fits. The amplitude A_k is the only fit parameter. In Supplementary Figure 5b, we plot the normalized amplitudes of Gaussian fits from Figure 5a as histograms. The data shows the probability within a laser pulse to detect 0, 1, 2 or more photons. These probabilities are fitted with Poisson distributions (stars) in order to obtain the average number of photons detected within a pulse, $\bar{n}$. We obtain a very good fit to experimental data with errors well below the standard deviation (i.e., $\sqrt{\bar{n}}$). The average detected photon-number obtained confirms the estimated absorbed photon rates.

We note that the dark current distribution is dominated by dark counts, which occur at a rate comparable to the measurement time. At faster operation speed of the photodiode,

© 2012 Macmillan Publishers Limited. All rights reserved.

the dark current would be dominated by the minority carrier drift current[3] that we assign to the peak at 0.48 pA.

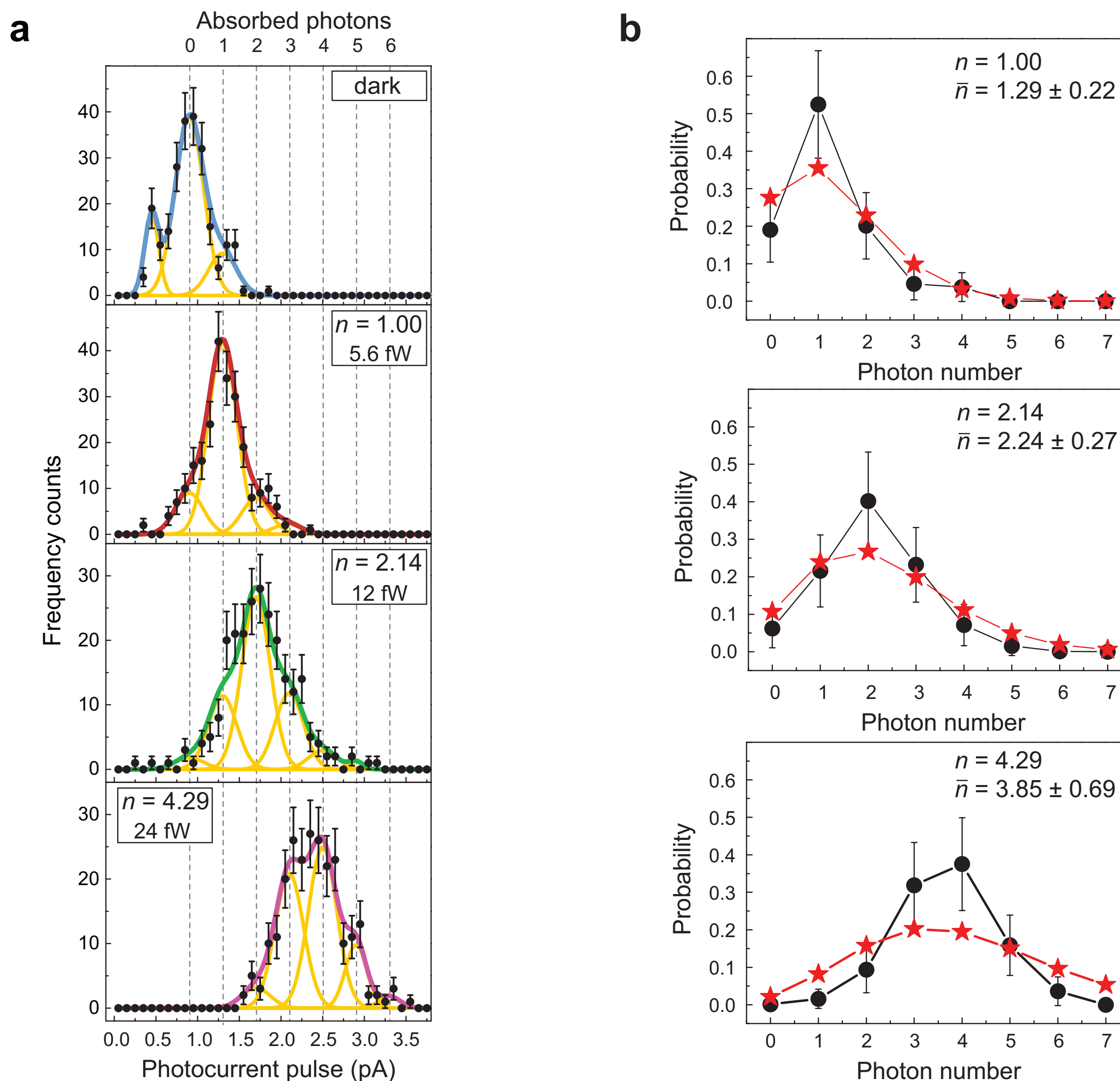

Figure 5: Photon counting measurements in the few-photon regime. **a**, The statistical distribution of current measured after individual excitation pulses with estimated absorbed photon number, n. Gaussian fits (yellow curves) to the data (black circles) are equally separated by 0.4 pA, which corresponds to the current generated by a single photon absorbed. The sum of Gaussian peaks assigned to the absorption of single photons is displayed by the colored curves. **b**, The normalized amplitude of Gaussian fits (circles) is very well described by Poisson distributions (stars) with average photon number $\bar{n}$, which confirms our estimations.

© 2012 Macmillan Publishers Limited. All rights reserved.

DOI: 10.1038/NPHOTON.2012.110

Measurement of doping concentrations

The doping concentrations were measured separately on homogenous n-doped and p-doped InP nanowires by four-terminal resistivity measurements, where nanowire dimensions were determined through SEM analysis. Homogenous n- and p-doped nanowires were grown under the same growth conditions as the experimentally investigated nanowire p-n junction. Contacts to n-doped InP nanowires are ohmic and a doping level of $10^{18}\,\mathrm{cm}^{-3}$ is obtained. Due to the Schottky nature of the p-contacts, current-voltage characteristics of homogenously p-doped nanowires are highly non-linear. The resistivity of the nanowire without contact contributions was measured using a four-terminal resistivity measurement. Supplementary Figure 6a shows a scanning electron micrograph of a single homogenously p-doped InP nanowire with four contacts. The two-terminal electrical characteristic of the p-InP nanowire is shown in Supplementary Figure 6b, whereas Supplementary Figure 6c shows the resistivity of only the nanowire without contact contribution measured by driving a current through contacts 1-4 and measuring the voltage drop at contacts 2-3 ($\Delta V_{2,3}$). From the measured resistance of $470\,\Omega$, we obtain a resistivity $\rho = R \cdot \frac{l}{S} = 63\Omega{\cdot}\mathrm{cm}$, which suggests a doping concentration of $10^{17}\,\mathrm{cm}^{-3}$ for the p-doped nanowires. The length (l) and the cross-section (S) of the nanowire are measured by SEM imaging, assuming a circular shape. Bulk InP values were used for both electron and hole mobilities[1]. From the measured doping levels we estimate a p-n junction depletion region width of 140 nm at zero applied bias, $V_{sd} = 0\,\mathrm{V}$. The depletion region width scales with the applied bias as $\sqrt{V_{bi} - V_{sd}}$, where V_{bi} is the built-in potential of the p-n junction and is approximately equal to the energy band-gap of the semiconductor[2]. As a result, the depletion region width increases up to 370 nm when the nanowire is biased at $V_{sd} = \text{-}8\,\mathrm{V}$.

© 2012 Macmillan Publishers Limited. All rights reserved.

DOI: 10.1038/NPHOTON.2012.110

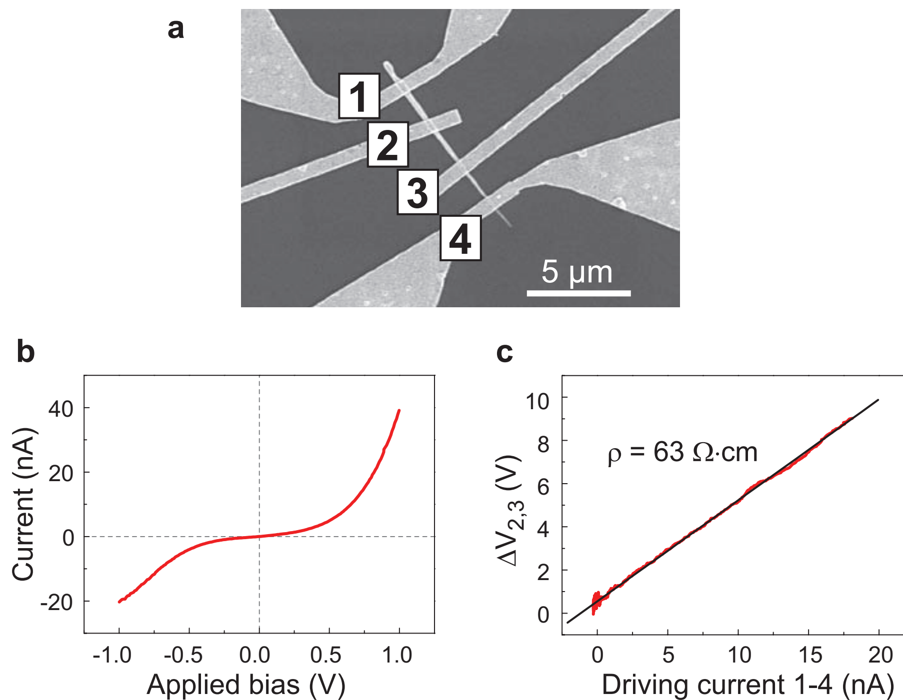

Figure 6: Measurement of p-doping concentration. **a**, Scanning electron micrograph of a single homogenously p-doped InP nanowire with four contacts. **b**, The non-linear two terminal I-V characteristic suggests the presence of Schottky contacts. **c**, The resistivity of the nanowire without the contact contribution is measured with a four-terminal electrical measurement. From the measured resistivity $\rho = 63\,\Omega{\cdot}\mathrm{cm}$, we obtain a doping concentration of $10^{17}\,\mathrm{cm}^{-3}$.

© 2012 Macmillan Publishers Limited. All rights reserved.

DOI: 10.1038/NPHOTON.2012.110

Estimation of the multiplication gain

In the presence of avalanche multiplication of charges, we observe that the absorption of a single photon yields 2.3×10^4 electrons and holes. From the impact ionization energy threshold $\varepsilon_e = 1.84\,\text{eV}$ for electrons and $\varepsilon_h = 1.65\,\text{eV}$ for holes, and the strength of the electric field, E, we calculate the number of impact ionization processes an electron or a hole undergoes in the nanowire depletion region. The distance that a carrier should ballistically travel through the crystal before gaining enough energy to overcome the ionization threshold and thus, generating an electron-hole pair is called the dead space[4], defined as:

$$d_{e,h} = \frac{\varepsilon_{e,h}}{eE}. \tag{3}$$

Here e is the electron charge. At saturation of the avalanche process, we calculate an electric field of $350\,\text{kV/cm}$ and a dead space of $d_e = 53\,\text{nm}$ for electrons and $d_h = 47\,\text{nm}$ for holes. Hence, in a depletion region of $370\,\text{nm}$, an electron (hole) undergoes seven (eight) impact ionization processes. After each impact ionization event, the carriers double.

In our estimation of the gain, we assume that the avalanche process initiates with an electron-hole pair at the edge of the depletion region close to the n-side. The electron is accelerated across the depletion region by the applied electric field and generates 2^7 electron-hole pairs by impact ionization. Since holes also contribute to the avalanche, the 2^7 generated holes undergo eight impact ionization events by traversing the depletion region towards the p-doped side. The final result is that a single optical excitation generates $2^7 \times 2^8 = 2^{15} = 3.3 \times 10^4$ electrons and holes. The measured gain of 2.3×10^4 agrees very well with the predicted gain in this simple picture. The same model holds for a multiplication process initiated from the p-side of the depletion region. We note that such a high gain is obtained because both carriers contribute to the multiplication process.

© 2012 Macmillan Publishers Limited. All rights reserved.

DOI: 10.1038/NPHOTON.2012.110

Polarization anisotropy

A comparison of the photocurrent measured as a function of incident light polarization angle for above bandgap excitation ($\lambda = 532$ nm) and resonant quantum dot p-shell excitation ($\lambda = 986$ nm) is shown in Supplementary Figure 7a. As typically observed in nanowires, the nanowire acts as a dielectric antenna for incoming light and thus photons polarized along the nanowire are favorably absorbed[5,6]. We observe this antenna effect both for excitation in the entire nanowire active area (crosses) and for selective excitation in the quantum dot (circles). The orientation of the nanowire is displayed by the dashed green line in the photocurrent scan in Supplementary Figure 7b. For all photocurrent measurements in the few-photon regime, the laser polarization was aligned along the nanowire axis, where the absorption is maximum. The estimated absorption coefficients are only valid for polarization along the nanowire axis, as the absorption is strongly suppressed for perpendicular polarization components by the nanowire antenna effect.

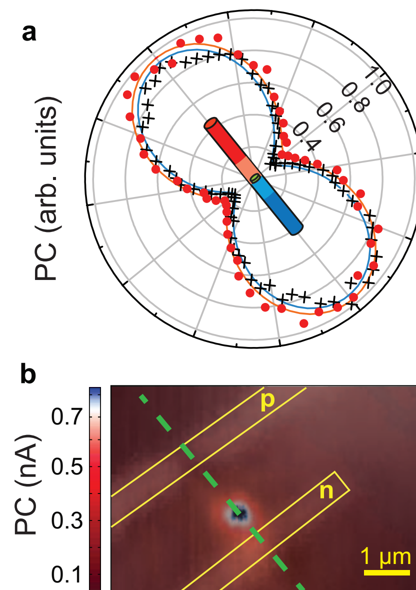

Figure 7: **a**, Measurement of the linear polarization sensitivity for excitation at $\lambda = 532$ nm (blue fit to crosses) and resonant excitation in the quantum dot (red fit to circles). In both cases, the maximum absorption is obtained for light polarized along the nanowire axis. **b**, The dashed green line in the photocurrent image shows the nanowire orientation with respect to the contacts.

© 2012 Macmillan Publishers Limited. All rights reserved.

DOI: 10.1038/NPHOTON.2012.110

[1] Siegel W., Kühnel G., Koi H., Geelach W. Electrical properties of n-type and p-type InP grown by the synthesis, solute diffusion technique. *Phys. Stat. Sol. (a)*, **95**, 309, (1986).

[2] Sze S. M. *Physics of semiconductor devices.* (Wiley, New York, 1981).

[3] Kardynal B. E. , Yuan Z. L. and Shields A. J.. An avalanche-photodiode-based photon-number-resolving detector. *Nature Photon.*, **2**, 425–428 (2008).

[4] McIntyre, R.J. Multiplication noise in uniform avalanche diodes," IEEE Trans Electron. Dev. **13**, 164–168 (1966).

[5] Wang J., Gudiksen M. S., Duan X., Cui Y. and Lieber C. M. Highly polarized photoluminescence and photodetection from single indium phosphide nanowires. *Science*, **293**, 1455–1457, (2001).

[6] van Kouwen M. P., et al. Single quantum dot nanowire photodetectors. *Appl. Phys. Lett.*, **97**, 113108, (2010).

© 2012 Macmillan Publishers Limited. All rights reserved.